Isotope effects in the electronic structure of PdH_x and PdD_x from de Haas–van Alphen measurements

H. L. M. Bakker, R. Feenstra, R. Griessen, L. M. Huisman, and W. J. Venema
Natuurkundig Laboratorium der Vrije Universiteit, Amsterdam, The Netherlands
(Received 14 June 1982)

The concentration dependence of extremal cross-sectional areas of the Fermi surface of dilute PdH_x and PdD_x alloys ($0 \leq x \leq 0.005$) has been determined from de Haas–van Alphen measurements in fields up to 10.5 T. The data confirm the general features of the proton model: States at the Fermi level are lowered in energy and the electrons added to the metal by the dissolved hydrogen or deuterium are partially accommodated at the Fermi surface of the host. The de Haas–van Alphen measurements show for the first time that large isotope effects are present in the concentration dependence of some of the Fermi-surface sheets. The sheets that show the largest isotope effect are those that contain mostly states with a vanishing charge density at the hydrogen site. The experimental results are discussed in terms of a proton screening potential exhibiting a Thomas-Fermi behavior at short distance and Friedel-type oscillations at large distance.

I. INTRODUCTION

The critical temperature T_c for the superconducting transition in PdH_x and PdD_x is known[1] to increase rapidly with hydrogen or deuterium concentration for $x \gtrsim 0.8$. In the stoichiometric alloys $T_c(\mathrm{PdH}) \cong 9$ K and $T_c(\mathrm{PdD}) \cong 11$ K. Two mechanisms have been proposed so far to explain the inverse isotope effect in T_c. According to Miller and Satterthwaite[2] the difference between the amplitude of the zero-point motion of a proton and that of a deuteron at the interstitial sites of palladium is responsible for a difference in the electronic structure of PdH_x and PdD_x. These authors did not, however, evaluate quantitatively the effect of zero-point motion on the electronic structure of these alloys.

Ganguly[3] and later Papaconstantopoulos *et al.*[4] and Klein *et al.*[5] take almost the opposite point of view. They assume that the electronic structures of PdH_x and PdD_x are the same but that the contribution of the optical phonons to the electron-phonon enhancement parameter λ depends on the zero-point motion of H (or D) via the anharmonicity of the H-Pd (or D-Pd) potential. Differences between the force constants $M_H\omega_H^2$ and $M_D\omega_D^2$ of H (or D) in Pd have been observed in neutron scattering,[6] superconductive tunneling,[7] Raman scattering,[8] electrical resistivity,[9,10] and elastic moduli measurements.[11] As an average one finds $M_H\omega_H^2/M_D\omega_D^2 \simeq 1.1$. Even with the highest anharmonicity, $M_H\omega_H^2/M_D\omega_D^2 \simeq 1.2$, deduced from a comparison of two different types of neutron scattering data,[6] Papaconstantopoulos *et al.*[4] find an inverse isotope effect that is still roughly two times smaller than the experimental value.[12] This indicates that anharmonicity of the proton-palladium potential alone is not sufficient to explain the differences in the T_c of PdH_x and PdD_x.

In the last few years several models that combine differences in both the force constant and the electronic structure have been proposed. Karakozov and Maksimov[13] conclude that the most important mechanisms that influence λ are the renormalization of phonon frequencies and the Debye-Waller factor in the electron-phonon matrix elements due to the zero-point motion of the interstitial. The effect of hybridization between *s*- and *d*-electron states on the superconductivity of PdH_x and PdD_x is investigated by Morozov.[14] Both the models of Karakozov and Maksimov and of Morozov lead to an increase of λ_{PdD_x} relative to λ_{PdH_x}. Quantitative calculations using realistic band structures have, however, not been carried out so far.

Measurements of T_c or other physical quantities such as the electronic specific heat, low-temperature thermal expansion, electrical resistivity, or spin-lattice relaxation are not detailed enough to identify unambiguously the origin of the inverse isotope effect. Furthermore, the resolution of present available spectroscopic methods (photoemission, Raman scattering, superconductive tunneling) is not high enough to detect differences of the order ~ 1 mRy in the electronic structure of PdH_x and PdD_x.

This provided us with the motivation to study the Fermi surface of PdH_x and PdD_x by means of the de Haas–van Alphen effect. Although this

quantum-oscillations technique can only be used for dilute hydrides and deuterides and will therefore provide us with results that are not *directly* applicable to the highly concentrated superconducting hydrides and deuterides, it has the great advantage of being very sensitive to changes in the band structure at the Fermi energy. In materials such as PdH_x and PdD_x, where the Fermi surface consists of various sheets, quantum-oscillatory measurements make it also possible to investigate the influence of H (or D) on electron states with a rather well-defined symmetry character. As shall be shown the large isotope effects found for electron states with a strongly *d* character and the absence of such effects for *s* electrons is an important result that indicates that the electronic structure of PdH_x and PdD_x is in fact influenced by the amplitude of the zero-point motion of the proton or deuteron.

This paper is organized as follows. In Sec. II we describe the preparation of the samples and the experimental techniques used to detect the small changes between the Fermi surface of PdH_x and that of PdD_x. Experimental results for $d\ln A/dx$, the relative change of an extremal cross sectional area A of the Fermi surface with hydrogen or deuterium concentration x, are presented in Sec. III and discussed in Sec. IV.

II. EXPERIMENT

A. Experimental methods

The changes of the Fermi surface of palladium due to the absorption of hydrogen or deuterium are measured by means of the de Haas–van Alphen (dHvA) effect. Two different methods, (i) the field-modulation technique and (ii) the torque method, are used in this work. For both methods the accuracy required to detect the small changes induced by H or D in the Fermi surface of Pd is obtained with the use of sample holders with accurate positioning facility and the dual dHvA spectrometers described below.

1. Field-modulation technique

The method used for dHvA measurements on small Pd, PdH_x, or PdD_x samples (typically $0.7\times0.7\times10$ mm^3) is the large-amplitude field-modulation technique. Since the method is described in great detail by Stark and Windmiller[15] we give here only a very brief description of our experimental setup. The sample holder is shown in Fig. 1. It consists of two dHvA detection systems: one for measurements on Pd (hydrogenated or not) and one for measurements of the dHvA signal of a copper reference crystal. The palladium sample is soldered to a beryllium-copper plunger with the use of a silver-based solder with a melting point of 550 °C. The plunger can be taken out of the sample holder for hydrogenation or deuteration. The reproducibility in the position of the Pd crystal before and after H (or D) loading is checked by means of the dHvA effect itself; the relative changes in the frequencies after removal and subsequent repositioning of the sample are less than 10^{-5}.

For all runs the modulation frequency lies between 30 and 90 Hz. The skin depth is then much larger than the diameter of the sample. A PDP 11/05 computer monitors the magnet current, which is proportional to the magnetic induction B, and adjusts the field-modulation amplitude b in such a way that the modulation phase factor b/B^2 remains constant. The signal induced in the pickup coil is fed via a low-noise impedance-matching transformer to a lock-in amplifier for phase-sensitive detection. Second-harmonic detection is used for most of the measurements.

In order to obtain the accuracy required to measure the small dHvA frequency changes induced by H or D in Pd we use the method of Harmans and

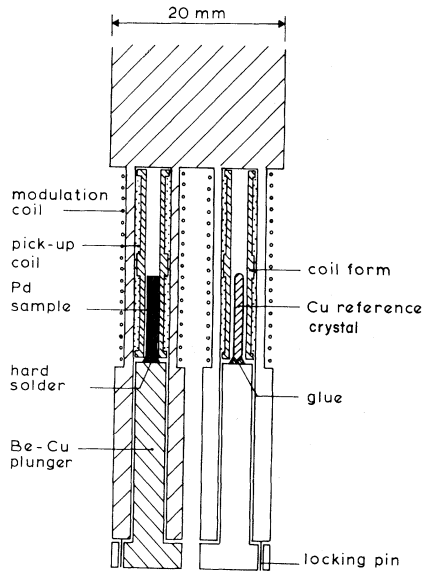

FIG. 1. Sample holder for the dHvA experiments using the field-modulation technique. The dHvA signal of the copper reference crystal is used to calibrate continuously the magnetic field.

Lassche[16] for the calibration of the magnetic field. Calibration points equidistant in $1/B$ are obtained by means of the reference detection system shown in Fig. 1. The reference crystal is a copper crystal with a relatively high Dingle temperature. The copper dHvA signal is almost free of harmonic content. The negative-to-positive zero crossings of the reference signal are used for the timing of the data sampling of the Pd, PdH_x, or PdD_x signals. The magnetic field is varied at constant $d(1/B)/dt$. The copper [111]-neck frequency $F=2173.56$ T is used to measure the X and L pockets of palladium, and the [111]-belly frequency $F=58\,072.4$ T is used to measure the large palladium Γ electron sheet.

2. *de Haas—van Alphen torque*

A schematic diagram of the torquemeter used for dHvA measurements on large samples (typically $6\times6\times10$ mm^3) is shown in Fig. 2. It is a modified version of the one used by Griessen *et al.*[17] It consists of a movable part (on which the Pd sample is attached) supported by a double crossed-spring system. The rotation axis of the movable part is perpendicular to the magnetic field B and parallel to the [010] axis of the investigated Pd, PdH_x, or PdD_x crystals. The whole torquemeter can be rotated about an axis parallel to the rotation axis of the movable part, so that the direction of B can be varied in the (010) plane. The position of the sample is accurately reproduced by clamping it on the spring-suspended movable part of the torquemeter. The whole torquemeter is subsequently aligned in the magnetic field by observing the beat pattern of the dHvA oscillations of the X ellipsoids near [110].

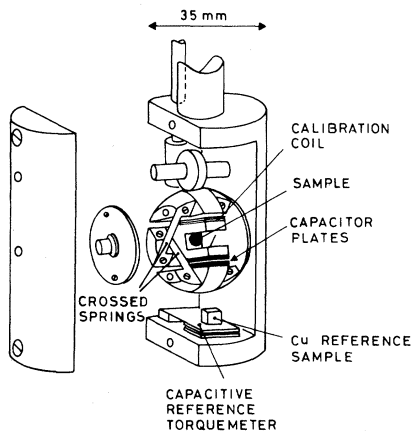

FIG. 2. Torquemeter used for dHvA measurements.

The very small rotation of the movable part produced by the dHvA torque changes the distance between the two capacitor plates; the resulting capacitance changes are measured with a General Radio capacitance bridge. Similar to the field-modulation technique the data acquisition of the palladium signal is triggered by the dHvA signal of a copper reference crystal. This copper crystal is cut approximately 5° off the [111] direction and is mounted on a miniaturized capacitance torsion balance.

The merits of the field-modulation technique are its high sensitivity and the possibility to suppress unwanted dHvA frequencies or harmonics by choosing an appropriate modulation amplitude. The main advantage of the torque method, on the other hand, is that absolute measurements can be done on relatively large samples without encountering skin-depth problems. This is important for our investigation of PdH_x and PdD_x as it makes it possible to use samples for which the hydrogen or deuterium concentrations can be accurately determined gravimetrically. For high dHvA frequencies the sensitivity of the torque method is, however, lower than that of the field-modulation technique. The torque method is thus used only for measurements of the H- or D-concentration derivatives $d\ln A/dx$ of extremal cross sections of the X and L hole ellipsoids. The field-modulation technique is primarily used to measure the *ratios* of the $d\ln A/dx$ derivatives for the Γ, X, and L orbits.

Both the field-modulation and torque dHvA spectrometers fit into the bore of a multifilamentary Nb_3Sn-NbTi superconducting magnet of 12-T maximum field. The homogeneity is better than 10^{-5} in a sphere of 15-mm diameter. All the field sweeps were carried out between 4 and 10.5 T at temperatures between 1.2 and 1.5 K.

The dHvA frequencies and amplitudes averaged over the magnetic field range of a given "field-modulation" or "torque" run are determined by means of standard Fourier transformation or from a least-squares fit of the data by means of de Prony's method[18] (for a recent description of this method see Ref. 19). With both methods of analysis the frequencies are reproducible within one part in 10^6 from run to run.

B. Sample preparation

The palladium samples used in this work are prepared from palladium powder with a total quoted impurity content of 6 ppm (less than 2 ppm iron) supplied by Johnson and Matthey. The powder is

melted in a water-cooled copper boat with the use of high-frequency induction heating to obtain a rodlike ingot. From this ingot a cylindrical single crystal with a diameter of ~ 7 mm and a length of ~ 80 mm is grown by means of zone melting and subsequently cut by means of spark erosion into rectangular bars of $0.7\times 0.7\times 10$ mm^3 for field-modulation measurements, and cylindrical samples with a diameter of 6 mm and a length of 10 mm are cut for torque measurements. The samples are etched in dilute aqua regia to obtain a clean surface and annealed in air for 72 h at 1000 °C. The final resistivity ratio $\rho(300\ \mathrm{K})/\rho(4.2\ \mathrm{K})$ is approximately 6000.

The Pd crystals are charged with H or D by gas absorption at a temperature between 470 and 670 K. The equilibrium gas pressure required for a desired concentration is evaluated for the low-concentration limit[20] by means of

$$[p(\mathrm{Torr})]^{1/2}=x\exp[C_1+(C_2/k_BT)] \qquad (1)$$

with the values $C_1=9.77$ and $C_2/k_B=-1165$ K for PdH_x, and $C_1=9.72$ and $C_2/k_B=-950$ K for PdD_x, given by Wicke and Nernst.[21] k_B is the Boltzmann constant and x is the concentration of interstitials. In order to obtain a uniform concentration (deviation less than 1% of the average concentration) the samples are kept at the loading temperature for a time longer than $R^2/D_{\mathrm{H(D)}}$ where R is the radius of the sample and $D_{\mathrm{H(D)}}$ is the hydrogen (deuterium) diffusion coefficient at the loading temperature.

After charging, the concentration of the large samples used in torque experiments is accurately determined by measuring the weight increase due to the hydrogen or deuterium uptake with a Mettler microgram balance. The reproducibility of the gravimetric measurements is ~ 1 μg. The corresponding uncertainty $\Delta x/x$ is about 8%. As shown in Fig. 3 good agreement is found between the predictions of Eq. (1) and the concentrations determined gravimetrically.

One of the major difficulties of the present dHvA investigation is to produce *homogeneous* dilute α-phase PdH_x and PdD_x samples *at liquid-helium temperatures.* The difficulty is that the coexistence line between the homogeneous α and the mixed $(\alpha+\alpha')$ phases of the PdH_x or PdD_x phase diagrams[23] is inevitably crossed when cooling the sample down from the temperature of ~ 600 K, at which the sample is charged with H or D, to the temperature of ~ 1.5 K, at which dHvA experiments are carried out. At that temperature and in

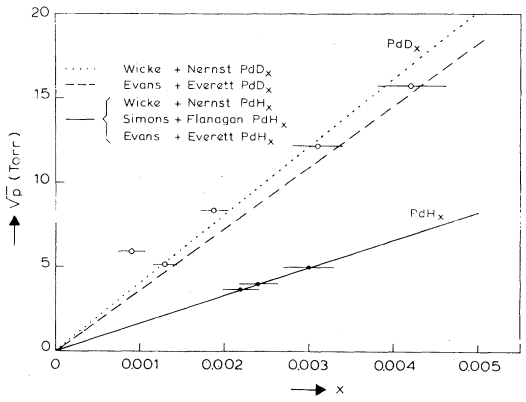

FIG. 3. Sieverts plot for the PdH_x and PdD_x samples used in dHvA torque measurements. The samples are charged with hydrogen at 498 K and with deuterium at 673 K. [See Wicke *et al.* (Ref. 21), Evans *et al.* (Ref. 24), and Simons *et al.* (Ref. 22).]

thermodynamical equilibrium the sample consists of islands of concentrated α'-phase $PdH_{0.66}$ ($PdD_{0.66}$) in a virtually pure palladium matrix. Depending on the cooling rate from ~ 600 K to helium temperatures the segregation in α and α' phases will be more or less complete.

The effect of phase segregation on the dHvA frequency corresponding to the smallest cross-sectional area of the X ellipsoid is shown in Fig. 4. The frequency varies in a complicated way with concentration. At low concentrations ($x<0.005$) the frequency decreases linearly with the hydrogen-to-palladium ratio. At concentrations higher than

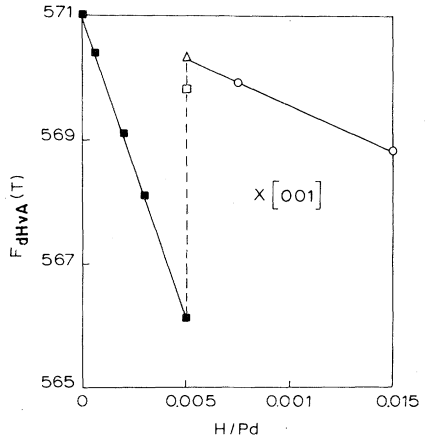

FIG. 4. Variation of the dHvA frequency of the [001] orbit of the hole ellipsoid centered at $X(0,0,1)$ with hydrogen concentration x. For $x=0.005$ the frequency shifts are strongly dependent on the cooling rate. Cooling rate: 1200 K/min (■); 30 K/min (□); 10 K/min (△); 2 K/min (○).

0.005 the frequency decreases linearly too, but with a significantly smaller slope. The frequency shifts observed around $x=0.005$ depend strongly on the rate at which the sample is cooled down.

This indicates that a homogeneous α phase can be obtained by rapidly cooling down samples containing no more than 0.5 at. % hydrogen at a rate of 1200 K/min. For higher concentrations segregation takes place because the diffusion rate at the temperature T_{coex}, where the α-α'—phase coexistence line is crossed, is much higher than in very dilute samples (T_{coex} tends to zero in the limit of low concentrations). The observed dHvA frequency shifts correspond then to a palladium-hydrogen alloy with a concentration equal to that of the nonequilibrium α-phase matrix (the contribution of the highly disordered α' islands that occupy only a small fraction of the sample volume is negligible). This concentration is lower than the nominal hydrogen concentration x in the sample, and therefore the observed variation with x is smaller than in a nonsegregated sample. The same behavior is observed for PdD_x alloys except that the maximum concentration for which homogeneous α-phase samples can be obtained by quenching at 1200 K/min is reduced to 0.4 at. % D. This is due to the higher diffusion rate of D in Pd (at room temperature, for example, the diffusion coefficient of D in Pd is 5.95×10^{-7} cm^2/s while that of H in Pd is 4.04×10^{-7} cm^2/s).

III. EXPERIMENTAL RESULTS

Detailed experimental dHvA studies by Vuillemin[25] and recently by Dye *et al.*,[26] as well as band-structure calculations by Mueller *et al.*,[27] Andersen and Mackintosh,[28] and Andersen[29] indicate that the Fermi surface of palladium consists of a sixth-band electron sheet centered at point Γ of the Brillouin zone, three equivalent fourth-band hole ellipsoids at X, four equivalent fifth-band hole ellipsoids at L, and a complex structure of interconnected tubes open along the [001] directions, the so-called fifth-band jungle gym. The principal cross-sectional areas of the Γ electron sheet and the X and L hole ellipsoids investigated in this study are indicated in Fig. 5. The H- and D-concentration dependence of the dHvA frequencies corresponding to the cross sections in Fig. 5 is shown in Figs. 6(a)—6(d) for *homogeneous* α-phase PdH_x and PdD_x alloys. For both the hydrides and the deuterides the frequency and therefore the size of the electron sheet at Γ increases with increasing interstitial concentration while the hole ellipsoids at X and L decrease in size. Values for $d\ln A/dx$ derived from the slope of the curves in Figs. 6(a)—6(d) are given in Table I. The data in Figs. 6(a)—6(d) or Table I show that *important isotope effects may be present in the electronic structure of metals containing light interstitials.* The concentration dependence of X and L hole ellipsoids in PdH_x is 2 to 3 times smaller than in PdD_x. On the other hand, *no isotope effect* is present for the Γ electron sheet. This indicates that isotope effects

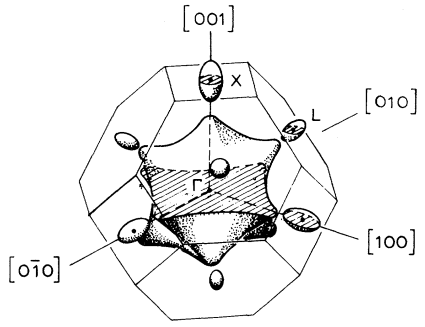

FIG. 5. Γ electron sheet and the X and L hole pockets of the Fermi surface of palladium. The investigated extremal cross-sectional areas are shaded.

TABLE I. Hydrogen- (deuterium-) concentration derivatives of the dHvA frequencies F associated with the extremal cross-sectional areas A shown in Fig. 5 ($F=\hbar cA/2\pi e$). The experimental methods used to obtain $d\ln F/dx$ are indicated by M (field modulation) or T (torque method).

Fermi-surface sheet	Orbit center	Field direction	F (T)	A (a.u.$^{-2}$)	$d\ln F/dx$ PdH_x	$d\ln F/dx$ PdD_x
Γ electron sheet	Γ(0,0,0)	[001]	27 330	0.7305	$+0.26\pm0.03$ (M)	$+0.24\pm0.03$ (M)
X hole pocket	X(0,0,1)	[001]	571	0.0153	-1.9 ± 0.2 (M,T)	-3.4 ± 0.3 (M,T)
	X(0,0,1)	[101]	689	0.0184	-1.7 ± 0.2 (T)	-3.7 ± 0.6 (T)
	X(1,0,0)	[001]	888	0.0237	-2.0 ± 0.2 (M,T)	-4.0 ± 0.4 (M,T)
L hole pocket	$L(\frac{1}{2},\frac{1}{2},\frac{1}{2})$	[001]	228	0.0061	-8 ± 1 (M,T)	-22 ± 1 (M,T)

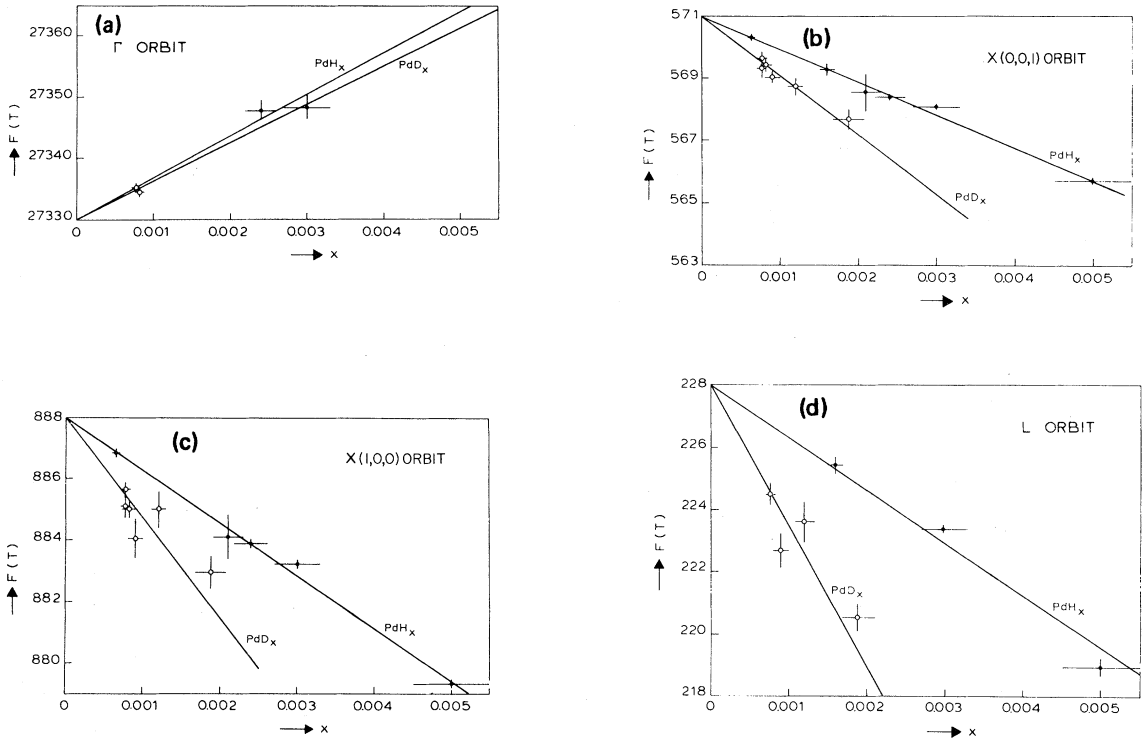

FIG. 6. Concentration dependence of the dHvA frequency of several extremal cross-sectional areas of Pd; (a) Γ orbit, (b) $X(0,0,1)$ orbit, (c) $X(1,0,0)$ orbit, and (d) L orbit. (●) PdH_x and (○) PdD_x.

are strongly dependent on the symmetry of the states at the Fermi surface of the host metal.

It is important to note here that in the present dHvA investigation of the Fermi surface of PdH_x and PdD_x, the H- (D-) concentration dependence of the Γ orbit is determined in the same run as that of the X and L orbit. The observed isotope effect for the X and L orbit can therefore not be due to a systematic experimental error, just as in the *same* run, on the *same* sample, no isotope effect is observed for the Γ orbit. Furthermore, isotope effects have been observed in both the absolute value (in torque measurements) and the ratios of $d\ln A/dx$'s (obtained from field-modulation runs).

Recently, isotope effects have also been found for the concentration dependence of the Dingle temperature T_D ($k_B T_D = \pi \Delta E$, where ΔE is the broadening of electronic levels by impurities). For the X ellipsoids dT_D/dx is approximately two times larger in PdD_x than in PdH_x. Within experimental error no isotope effect in dT_D/dx is observed for the Γ sheet.[30]

IV. ANALYSIS OF RESULTS

A. Reduction of experimental data

In the present section the experimental results given in Table I will be analyzed in detail. The frequency shifts associated with the dHvA orbits will be converted to average shifts in energy of the states on those orbits. In order to simplify the subsequent discussion we first separate volume effects from purely electronic contributions to the dHvA frequency shifts.

As is well known the macroscopic total volume increase $\Delta\Omega_{\text{tot}}$ of a sample absorbing hydrogen is partly due to the extra volume of the interstitial itself and partly to the relaxation of the host lattice. Only the latter contribution to the volume expansion will affect the dHvA frequencies. As calculated by Eshelby[31] the contribution of the metal-matrix relaxation $\Delta\Omega_{\text{mat}}$ to the total volume change caused by a homogeneous distribution of dilation centers is

$$\Delta\Omega_{\rm mat}=\frac{2}{3}\frac{1-2\nu}{1-\nu}\Delta\Omega_{\rm tot}\ ,$$

where ν is the Poisson ratio of the matrix. For palladium at low temperatures,[32] $\nu\equiv -S_{12}/S_{11}=0.435$. Together with $(d\ln\Omega/dx)_{\rm tot}=0.19$ (Refs. 33–35) this leads to a concentration dependence of the palladium-matrix expansion $(d\ln\Omega/dx)_{\rm mat}=0.03$, which is only 16% of the total volume expansion. The dHvA frequency shifts at constant volume Ω are thus given by

$$\left.\frac{\partial\ln F}{\partial x}\right|_{\Omega}=\frac{d\ln F}{dx}-0.03\left.\frac{\partial\ln F}{\partial\ln\Omega}\right|_{x}\ .$$

The volume derivatives of the dHvA frequencies were measured in Pd by Venema *et al.*[36] We assume here that they are independent of x for small x. For all orbits the volume-dependent term is small.

We can now convert the volume-corrected frequency shifts $(\partial\ln F/\partial x)_{\Omega}$ to energy shifts $\Delta E\equiv\langle E_{\vec{k}}-E_F\rangle$ at constant volume by means of

$$\frac{\Delta E}{x}=\frac{A}{\pi m_b}\left.\frac{\partial\ln F}{\partial x}\right|_{\Omega} \tag{2}$$

if one assumes that $d\ln m_b/dx\approx 0$. The angular brackets indicate an average over the orbit associated with the frequency F. A is the area of the corresponding extremal cross section and m_b the band mass. For small values of x, E_F remains constant relative to the atomic zero of energy. Therefore, in the dilute limit ΔE is the energy shift on an absolute energy scale.

The energy shifts calculated by means of Eq. (2) are given in Table II. This table shows that the Γ sheet is pulled down at the rate $\Delta E/x=45\pm 2$ mRy in both PdH_x and PdD_x. The small difference between the hydrides and the deuterides is less than the experimental error. The X and L pockets, on the other hand, are seen to behave completely differently in the hydride and the deuteride. In PdH_x both are pulled down by 20–25 mRy per H, while in PdD_x they are lowered by 45 and 65 mRy per D, respectively.

TABLE II. Hydrogen- (deuterium-) concentration derivatives at constant volume of average energy shifts $\Delta E/x$ (in mRy) for various orbits of the Fermi surface of PdH_x and PdD_x. The values for the X orbit are averages over the measured orbits indicated in Table I.

	$\Delta E/x$ (mRy)	
Orbit	PdH_x	PdD_x
Γ	-47 ± 5	-43 ± 5
X	-23 ± 2.4	-45 ± 4
L	-23 ± 2.9	-64 ± 2.5

B. Semirigid band model

The results for the Γ sheet can be used to obtain more information on the influence of H or D on the electronic structure of the Pd host. To this end we describe the electronic structure of PdH_x or PdD_x by three bands: a nearly-free-electron band, a d band, and a low-lying H (D) band. The last one vanishes in the limit of $x=0$. Furthermore, we assume that the nearly-free-electron band and the d band are shifted rigidly in energy by amounts $x\delta_c$ and $x\delta_d$, respectively (see Fig. 7). We also assume that these two bands lose some weight in favor of the H (D) band when H or D is added. The corresponding densities of states $n_c(\epsilon)$ and $n_d(\epsilon)$ can then be written to lowest order in x as

$$n_c(\epsilon)=[1-x\gamma_c(\epsilon)]n_c^0(\epsilon-x\delta_c)\ , \tag{3a}$$

$$n_d(\epsilon)=[1-x\gamma_d(\epsilon)]n_d^0(\epsilon-x\delta_d)\ , \tag{3b}$$

where n_c^0 and n_d^0 are the densities of states of the nearly-free-electron band and of the d band, respectively. $\gamma_c(\epsilon)$ and $\gamma_d(\epsilon)$ describe the loss of weight of these bands. Volume effects such as band narrowing do not need to be considered here since the energy shifts at *constant volume* are being discussed.

The number of states ζ pulled below E_F by the rigid shifts $x\delta_c$ and $x\delta_d$ is equal to the number of electrons put at the Fermi surface when H or D is added. This can be estimated from band-structure calculations[37] or magnetic susceptibility measurements.[23,39] In the semirigid band model ζ is equal

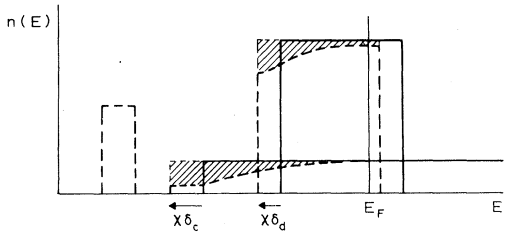

FIG. 7. Model density of states of Pd (——) and PdH_x (---). The shaded area indicates the part of the density of states of Pd that has disappeared due to the addition of hydrogen. Its weight is equal to that of the low-lying hydrogen band ($=2x$).

to

$$\zeta = \int_{E_F}^{E_F - x\delta_d} n_d^0(\epsilon)[1 - x\gamma_d(\epsilon)]d\epsilon + \int_{E_F}^{E_F - x\delta_c} n_c^0(\epsilon)[1 - x\gamma_c(\epsilon)]d\epsilon = -x[n_d^0(E_F)\delta_d + n_c^0(E_F)\delta_c] + O(x^2) . \quad (4)$$

The loss of weight of the Pd bands does not contribute to ζ to first order in x.

The number of valence electrons per unit cell is given by

$$10 + x = 2x + \int_{-\infty}^{E_F} n_c(\epsilon)d\epsilon + \int_{-\infty}^{E_F} n_d(\epsilon)d\epsilon \quad (5)$$

since Pd has ten electrons and the hydrogen atoms contribute x electrons per unit cell. On the right-hand side of Eq. (5), $2x$ is the number of electrons in the low-lying impurity band. The other two terms are the number of electrons in the nearly-free-electron band and d band, respectively. With the use of Eqs. (3) and (5), Eq. (4) can be rewritten as

$$\frac{\zeta}{x} = \int_{-\infty}^{E_F} [n_c^0(\epsilon)\gamma_c(\epsilon) + n_d^0(\epsilon)\gamma_d(\epsilon)]d\epsilon - 1 . \quad (6)$$

Equation (6) shows that ζ/x is equal to the number of Pd valence electrons that are removed from the Pd bands due to the loss of weight of these bands, minus the number of Pd electrons accommodated in the low-lying band. In the anion model[40] it is assumed that the weight of the Pd bands does not change upon H absorption. This means that $\gamma_c(\epsilon)$ and $\gamma_d(\epsilon)$ vanish identically and that $\zeta/x = -1$. The proton model,[41] on the contrary, corresponds to the case where the hydrogen band is derived completely from Pd bands below E_F. This means that

$$2x = x\left[\int_{-\infty}^{E_F} n_c^0(\epsilon)\gamma_c(\epsilon)d\epsilon + \int_{-\infty}^{E_F} n_d^0(\epsilon)\gamma_d(\epsilon)d\epsilon\right] .$$

Therefore, in this model $\zeta/x = +1$. ζ/x is expected to lie between these limits. Averaged t-matrix calculations[37] have shown that the Pd bands lose weight in favor of the hydrogen band and that ζ/x is roughly equal to 0.5 in dilute PdH_x alloys. This result is confirmed by magnetic susceptibility measurements,[23] which indicate a value of roughly 0.6. Recent susceptibility measurements[39] also show that ζ/x is the same for both H and D.

Using Eq. (4) we can evaluate the average energy shift of the d band, δ_d, which is essentially equal to the average energy shift of the states on the jungle gym.[27,29] For this we need values for δ_c and for $n_d^0(E_F)$ and $n_c^0(E_F)$. δ_c is given in Table II (−47 mRy for PdH_x and −43 mRy for PdD_x). $n_d^0(E_F)$ and $n_c^0(E_F)$, calculated by Andersen,[29] are equal to 27.7 and 3.4 electron/Ry atom, respectively. The resulting relation between δ_d and ζ/x is shown in Fig. 8. The anion- and proton-model values of ζ/x are indicated, as well as the value estimated from the magnetic susceptibility measurements. The error bars arise from the 0.03 uncertainty in $(d\ln F/dx)_\Gamma$. They are very small because $\delta_c n_c^0(E_F)$ is of the order of 0.1.

The data given in Table II and the relationship between δ_d and ζ/x indicated in Fig. 8 lead to the following conclusions. The *relation* between δ_d and ζ/x is the same for both the hydride and the deuteride because, within experimental error, δ_c is the same for PdH_x and PdD_x. Furthermore, calculations[37,38] as well as experiments[23] indicate that $0.5 < \zeta/x < 1.0$. Magnetic susceptibility measurements,[39] moreover, indicate that ζ/x is isotope independent. As a result, δ_d is between −13 and −32 mRy and is the same in the hydride and the deuteride.

C. Isotope effect

Three features of the isotope effect have to be explained. In the first place, there is within experimental error no isotope effect in the shifts of the Γ states and consequently, as shown above, there is no isotope effect in the shifts of the energies of the jungle-gym states either. In the second place, there is a very large isotope effect for the small X and L

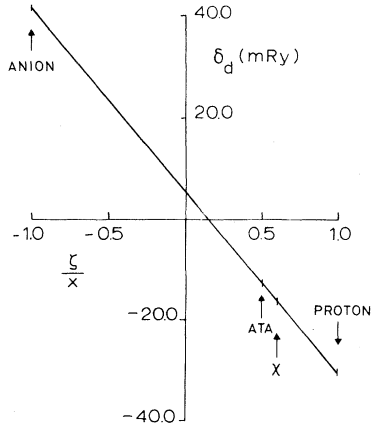

FIG. 8. δ_d as a function of ζ/x. The anion-model and proton-model values of ζ/x have been indicated, as well as estimates from averaged-t-matrix calculations (Ref. 38) and magnetic susceptibility (Ref. 39) measurements (X).

pockets. The difference in energy shift between the hydride and the deuteride is of the order of the energy shifts themselves. In the third place, there is a *qualitative* difference between the hydrides and the deuterides. In PdH_x all d states—small hole pockets and jungle gym—are shifted downwards by roughly the same amount (~ -20 mRy). If we take the energy shifts of the X and L pockets as a measure for the energy shift of all d states, i.e., as a measure for δ_d, then Eq. (4) would give for ζ/x a value of 0.8, which is not inconsistent with other estimates of this quantity. In PdD_x, however, the d states are shifted downwards at rates that depend *strongly* on the character of the states of interest (X pocket, L pocket, or jungle gym).

We attribute the isotope effect to the difference in mass between H and D, which in turn leads to a difference in the zero-point-motion amplitude of the interstitial in the Pd matrix. The energy of this zero-point motion is ~ 56 meV in PdH_x and ~ 40 meV in PdD_x.[42] Since these values are much lower than the plasma energy of the conduction electrons, which is of the order of 5 eV, the screening cloud around the impurity will follow the motion of the impurity adiabatically. The effective potential can then be written as $V(\vec{r}+\vec{\rho})$, where $\langle\rho^2\rangle$ is the momentary position of the impurity; its average value is determined by a Gaussian factor $e^{-3\rho^2/2\langle\rho^2\rangle}$, where $\langle\rho^2\rangle$ is the mean-square deviation of the impurity from its average position. From neutron scattering experiments[43] $\langle\rho^2\rangle$ is found to be equal to 0.32 a.u.^{2} in dilute hydrides and 0.23 a.u.^{2} in deuterides.

If $\langle\rho^2\rangle^{1/2}$ is small compared to a typical length of the potential, then $V(\vec{r}+\vec{\rho})$ can be expanded in a Taylor series around $\vec{\rho}=0$. The average potential is then the following:

$$\begin{aligned}\langle V(\vec{r})\rangle &= \left[\frac{3}{2\pi\langle\rho^2\rangle}\right]^{3/2} \\ &\quad\times\int e^{-(3/2)(\rho^2/\langle\rho^2\rangle)}V(\vec{r}+\vec{\rho})d\vec{\rho} \\ &= V(\vec{r})+\tfrac{1}{6}\langle\rho^2\rangle\nabla^2V(\vec{r})+\cdots . \end{aligned} \tag{7}$$

In the immediate vicinity of the impurity we can approximate $V(\vec{r})$ by

$$V(\vec{r})=-\frac{2}{r}\left[1+\frac{r}{2\lambda}\right]e^{-r/\lambda}, \tag{8}$$

in analogy with the time-averaged potential of a neutral hydrogen atom.[44] We also write the density $\varphi^*(\vec{r})\varphi(\vec{r})$, corresponding to the crystalline Pd state $\varphi(\vec{r})$ as

$$\varphi^*(\vec{r})\varphi(\vec{r})=|\varphi(\vec{o})|^2+g(\vec{r}),$$

where $|\varphi(\vec{o})|^2$ is the density at the octahedral site. To first order in $V(\vec{r})$ the energy shift ΔE is then equal to

$$\begin{aligned}\frac{\Delta E}{x} &= \int\langle V(\vec{r})\rangle\,|\varphi(\vec{r})|^2 d\vec{r} \\ &= -16\pi\lambda^2|\varphi(\vec{o})|^2 \\ &\quad+\int V(\vec{r})\left[1+\frac{1}{6}\frac{\langle\rho^2\rangle}{\lambda^2}f\left[\frac{\lambda}{r}\right]\right]g(\vec{r})d\vec{r}, \end{aligned} \tag{9}$$

with $f(\lambda/r)=(1+2\lambda/r)^{-1}$.

The energy shift $\Delta E_\Gamma/x$ of the states on the Γ sheet is dominated by the first term on the right-hand side of Eq. (9) because for these states $g(\vec{r})$ is small compared to $|\varphi(\vec{o})|^2$. By fitting λ to the observed value of $\Delta E_\Gamma/x$ (~ -45 mRy) we find that $\lambda\sim 0.58$ a.u. This value is close to that of the neutral hydrogen atom for which $\lambda_{\text{atom}}=0.5$ a.u.

Equation (9) shows that zero-point-motion effects are only possible when the charge density corresponding to state $\varphi(\vec{r})$ is not completely uniform. This is true in fact for all impurity potentials, not only those that allow a Taylor-series expansion, because the energy shift is independent of the position of the impurity when $\varphi^*(\vec{r})\varphi(\vec{r})$ is constant in space. The zero-point-motion effect occurs only in the factor $[1+\langle\rho^2\rangle/(6\lambda^2)]f(\lambda/r)$. As $\langle\rho^2\rangle$ is of order 0.3 a.u.^{2} and λ of order 0.6 a.u., this factor is roughly equal to 1.1. As a result, for states on the Γ sheet, the effect of zero-point motion is *at most* 10%. This is confirmed by the present dHvA experiments which show that within experimental error there is no isotope dependence of the Γ energy shifts.

The most interesting feature of the dHvA results, to be discussed now, is the isotope dependence of the energy shifts of the states on the X and L pockets. In analogy with Eq. (7) we can write $\Delta E/x$ as

$$\frac{\Delta E}{x}=\frac{\Delta E_\infty}{x}(1+\xi\langle\rho^2\rangle), \tag{10a}$$

with

$$\frac{\Delta E_\infty}{x}=\langle\varphi|V|\varphi\rangle \tag{10b}$$

and

$$\xi=\frac{\langle\varphi|\frac{1}{6}\nabla^2V|\varphi\rangle}{\langle\varphi|V|\varphi\rangle}. \tag{10c}$$

ΔE_∞ corresponds to the energy shift of an infinitely heavy interstitial.

For the X pocket, $\Delta E_\infty/x$ and ξ are found to be

equal to -89.2 mRy and -2.3 a.u.$^{-2}$, respectively. For the L pocket, the corresponding values are -176 mRy and -2.7 a.u.$^{-2}$. The large values of $\Delta E_\infty/x$ are difficult to understand because the X- and L-pocket states have virtually no charge density near the octahedral site. It is in fact negligible[45,46] out to about 2 a.u., which is far beyond the screening length $\lambda=0.58$ a.u. found above. As a result no short-range potential such as a muffin-tin potential can affect these states. This implies that the long-range part of the screened proton potential must be included in order to satisfy Friedel's self-consistency condition $dE_F/dx=0$. Some long-range effects such as those due to charge transfer may produce sizable energy shifts. These shifts are, however, the same for all d-like states and do not exhibit the strong $\vec{k}$ dependence implied by the present dHvA data.

Although the large absolute values obtained above for ξ cast some doubts on the validity of the expansion used in Eq. (10a) the negative sign of ξ suggests that the screening potential is oscillating in space rather than decreasing exponentially. This follows from the fact that for the potential given in Eq. (8) $\xi\simeq(6\lambda^2)^{-1}$, and consequently that $\xi<0$ implies that the screening length is imaginary.

In the remaining part of this section we shall explore the role of long-range oscillations in the screening potential. For simplicity we assume that the tails of the potential have the usual Friedel form

$$V(\vec{r})=C[\cos(2k_Fr+\eta)]/(k_Fr)^3\ ,$$

where the amplitude C, the phase η, and the Fermi-wave-vector k_F depend on the electronic structure of the host and on the scattering properties of the impurity.[47]

After averaging we find

$$\langle V(\vec{r})\rangle\sim\frac{C}{(k_Fr)^3}[1-\tfrac{1}{6}\langle\rho^2\rangle(2k_F)^2]\left[\cos(2k_Fr+\eta)+\tfrac{1}{3}\langle\rho^2\rangle(2k_F)^2\frac{\sin(2k_Fr+\eta)}{k_Fr}+O((k_Fr)^{-2})\right]. \quad (11)$$

The effect of zero-point motion occurs in two different places in the previous equation. First of all there is a multiplicative factor $1-\frac{1}{6}\langle\rho^2\rangle(2k_F)^2$, which is completely analogous to the factor $1+\frac{1}{6}\langle\rho^2\rangle f(\lambda/r)\lambda^{-2}$ in Eq. (9). In the simplest possible model the screening is done by the nearly-free conduction electrons, i.e., the Γ-sheet electrons. k_F is then of the order of 0.5 a.u.$^{-1}$ and C is of the order[48] of $(2\pi)^{-1}$. The multiplicative factor in Eq. (11) differs then from 1 by only a few percent and cannot explain the observed isotope effect.

Zero-point motion also enters the expression for $\langle V(\vec{r})\rangle$ through an extra term,

$$\Delta V=\tfrac{1}{3}C\langle\rho^2\rangle(2k_F)^2\frac{\sin(2k_Fr+\eta)}{(k_Fr)^4}\ .$$

This term is alternately attractive and repulsive with a wavelength $\pi/k_F\approx6$ a.u. By choosing η properly it can be made repulsive in the region where the d charge closest to the impurity is concentrated. As the strength of this term falls off as r^{-4}, subsequent attractive regions can be neglected.

For the states on the X pocket, which have nearly xz or yz symmetry, the resulting energy shifts can be easily computed by replacing the four lobes of the d states[49] by δ functions 1.0 a.u. away from the Pd atom. The large isotope effect can be reproduced by taking $k_F=0.5$ a.u.$^{-1}$ and $\eta=-1.1$. $|C|$, however, has then to be equal to 0.9 compared to $(2\pi)^{-1}$ in the free-electron model.

In conclusion, the isotope effect can, at least for the states on the X pocket, be reproduced by taking into account the long-range Friedel oscillations and the zero-point-motion-induced potential ΔV. Such an explanation is, however, quite unsatisfactory. We have shown above that the average shift of the d states is nearly isotope independent. It is not clear at all how this comes about with the use of the Friedel oscillations, because the perturbing potential ΔV is approximately constant in the region where the d charge is appreciable. Of course, the various d states do not have exactly the same spatial distribution and the required large $\vec{k}$ dependence of the energy shifts could be caused by a large spatial dependence of C and η. But even then, it is not clear physically why C and η should be such that in PdD_x the energy shifts of the states on the X and L pockets deviate strongly from the average shifts, while in PdH_x the energy shifts are all roughly equal. Another mechanism that takes these features explicitly into account seems to be called for.

ACKNOWLEDGMENTS

The authors would like to thank C. D. Gelatt, Jr., for making available to them the results of self-consistent band-structure calculations of Pd and PdH, and R. S. Sorbello for valuable discussions. They are grateful to the Stichting voor Fundamenteel Onderzoek der Materie for financial support of this work.

[1]R. W. Standley, M. Steinback, and C. B. Satterthwaite, Solid State Commun. 31, 801 (1979).
[2]R. J. Miller and C. B. Satterthwaite, Phys. Rev. Lett. 34, 144 (1975).
[3]B. N. Ganguly, Phys. Rev. B 14, 3848 (1976).
[4]D. A. Papaconstantopoulos, B. M. Klein, E. N. Economou, and L. L. Boyer, Phys. Rev. B 17, 141 (1978).
[5]B. M. Klein, E. N. Economou, and D. A. Papaconstantopoulos, Phys. Rev. Lett. 39, 574 (1977).
[6]A. Rahman, K. Sköld, C. Pelizzari, S. K. Sinha, and H. Flotow, Phys. Rev. B 14, 3630 (1976).
[7]B. Stritzker and H. Wühl, in *Hydrogen in Metals II,* edited by G. Alefeld and J. Völkl (Springer, Berlin, 1978), Chap. 6.
[8]R. Sherman, H. K. Birnbaum, J. A. Holy, and M. V. Klein, Phys. Lett. 62A, 353 (1977).
[9]P. Nédellec, L. Dumoulin, C. Arzoumian, and J. P. Burger, J. Phys. (Paris) Colloq. 39, C6-432 (1978).
[10]A. Gorska, A. M. Gorskii, J. Igalson, A. J. Pindor, and L. Sniadower, *Proceedings of the International Conference on Hydrogen in Metals, Paris, 1977* (Pergamon, London, 1977).
[11]B. M. Geerken, R. Griessen, L. M. Huisman, and E. Walker, Phys. Rev. B 26, 1637 (1982).
[12]V. B. Ginodman and L. N. Zherikhina, Fiz. Nizk. Temp. 6, 582 (1980) [Sov. J. Low Temp. Phys. 6, 278 (1980)].
[13]A. E. Karakozov and E. G. Maksimov, Zh. Eksp. Teor. Fiz. 74, 681 (1978) [Sov. Phys.—JETP 47, 358 (1978)].
[14]A. I. Morozov, Fiz. Nizk. Temp. 3, 235 (1977). [Sov. J. Low Temp. Phys. 3, 404 (1977)].
[15]R. W. Stark and L. R. Windmiller, Cryogenics 8, 272 (1968).
[16]C. J. P. M. Harmans and L. Lassche, J. Phys. E 10, 155 (1977).
[17]R. Griessen, M. J. G. Lee, and D. J. Stanley, Phys. Rev. B 16, 4385 (1977).
[18]R. de Prony, J. Éc Polytech. 1 (2), 24 (an. IV).
[19]J. R. Anderson, P. Heimann, W. Bauer, R. Schipper, and D. Stone, in *Proceedings of the International Conference on the Physics of Transition Metals, Toronto, 1977,* edited by M. J. G. Lee, J. M. Perz, and E. Fawcett (IOP, London, 1978), p. 81.
[20]J. R. Lacher, Proc. R. Soc. London Ser. A 161, 525 (1937).
[21]E. Wicke and G. H. Nernst, Ber. Bunsenges. Phys. Chem. 68, 224 (1964).
[22]J. W. Simons and T. B. Flanagan, J. Phys. Chem. 69, 3773 (1965).
[23]H. Frieske and E. Wicke, Ber. Bunsenges. Phys. Chem. 77, 50 (1973).
[24]M. J. B. Evans and D. H. Everett, J. Less Common Metals 49, 123 (1976).
[25]J. J. Vuillemin, Phys. Rev. 144, 396 (1966).
[26]D. H. Dye, S. A. Campbell, G. W. Crabtree, J. B. Ketterson, N. B. Sandesara, and J. J. Vuillemin, Phys. Rev. B 23, 462 (1981).
[27]F. M. Mueller, A. J. Freeman, J. O. Dimmock, and A. M. Furdyna, Phys. Rev. B 1, 4617 (1970).
[28]O. K. Andersen and A. R. Mackintosh, Solid State Commun. 6, 285 (1968).
[29]O. K. Andersen, Phys. Rev. B 2, 883 (1970).
[30]H. L. M. Bakker, R. Griessen, and L. M. Huisman (unpublished).
[31]J. D. Eshelby, J. Appl. Phys. 25, 255 (1954).
[32]E. Walker, J. Ortelli, and M. Peter, Phys. Lett. 31A, 240 (1970).
[33]H. Peisl, in *Hydrogen in Metals I,* edited by G. Alefeld and J. Völkl (Springer, Berlin, 1978).
[34]A. J. Maeland and T. B. Flanagan, J. Phys. Chem. 68, 1419 (1964).
[35]J. E. Schirber and B. Morosin, Phys. Rev. B 12, 117 (1975).
[36]W. J. Venema, H. Skriver, E. Walker, and R. Griessen, J. Phys. (Paris) Colloq. 39, C6-1099 (1978).
[37]C. D. Gelatt, Jr., H. Ehrenreich, and J. A. Weiss, Phys. Rev. B 17, 1940 (1978).
[38]A. Bansil, R. Prasad, S. Bessendorf, L. Schwartz, W. J. Venema, R. Feenstra, F. Blom, and R. Griessen, Solid State Commun. 32, 1115 (1979).
[39]E. Wicke (private communication).
[40]W. M. Mueller, J. P. Blackledge, and G. G. Libowitz, *Metal Hydrides* (Academic, New York, 1968), Chap. 6.
[41]Y. Ebisuzaki and M. O'Keeffe, Prog. Solid State Chem. 4, 187 (1967).
[42]J. J. Rush, International Symposium on the Electronic Structure and Properties of Hydrogen in Metals, Richmond, 1982 (Plenum, New York, in press).
[43]W. Drexel, A. Murani, D. Tocchetti, W. Kley, I. Sosnowska, and D. K. Ross, J. Phys. Chem. Solids 37, 1135 (1976). The value of $\langle \rho^2 \rangle$ for PdD_x was obtained by dividing the result for PdH_x by $\sqrt{2}$.
[44]This is a reasonable approximation for hydrogen in Pd. See B. M. Klein and W. E. Pickett, International Symposium on the Electronic Structure and Properties of Hydrogen in Metals, Richmond, 1982 (Plenum, New York, in press).
[45]W. J. Venema, thesis, Vrije Universiteit Amsterdam, 1980 (unpublished).

[46]R. Griessen and L. M. Huisman, International Symposium on the Electronic Structure and Properties of Hydrogen in Metals, Richmond, 1982 (Plenum, New York, in press).
[47]G. Grüner and M. Minier, Adv. Phys. 26, 231 (1977).
[48]J. S. Langer and S. H. Vosko, J. Phys. Chem. Solids 12, 196 (1959).
[49]W. A. Harrison, *Electronic Structure and the Properties of Solids* (Freeman, San Francisco, 1980), Chap. 19c.